Lunar Seismicity, Structure, and Tectonics

Author(s): D. R. Lammlein

Source: *Philosophical Transactions of the Royal Society of London. Series A, Mathematical and Physical Sciences*, Mar. 31, 1977, Vol. 285, No. 1327, The Moon: A New Appraisal from Space Missions and Laboratory Analyses (Mar. 31, 1977), pp. 451-461

Published by: Royal Society

Stable URL: https://www.jstor.org/stable/74874

Phil. Trans. R. Soc. Lond. A. **285**, 451–461 (1977) [451]
Printed in Great Britain

VI. THE PRESENT DAY MOON: ITS INTERNAL PROCESSES

Lunar seismicity, structure, and tectonics

By D. R. Lammlein
Pennzoil Company, Houston, Texas, U.S.A.

[Plate 1]

Interpretation of lunar seismic data results in a lunar model consisting of at least four and possibly five distinguishable zones: (I) the 50–60 km thick crust characterized by seismic velocities appropriate for plagioclaise rich materials, (II) the 250 km thick upper mantle characterized by seismic velocities consistent with an olivine-pyroxene composition, (III) the 500 km thick middle mantle characterized by a high Poisson's ratio, (IV) the lower mantle characterized by high shear-wave attenuation, and possibly (V) a core of radius between 170 and 360 km characterized by a greatly reduced compressional wave velocity. The Apollo seismic network detects several thousand deep moonquake signals annually. Repetitive signals from 60 deep moonquake hypocentres can be identified. The occurrence characteristics of the moonquakes from the individual moonquake hypocentres are well correlated with lunar tidal phases and display tidal periodicities of 1 month, $7\frac{1}{2}$ months, and 6 years. With several possible exceptions, the deep moonquake foci located to date occur in three narrow belts on the near side of the Moon, and are concentrated at depths of 800–1000 km. The locations of 17 shallow moonquake foci, although not as accurate as those of the deep foci, show fair agreement with the deep moonquake belts. Focal depths calculated for the shallow moonquakes range from 0–300 km. The moonquakes of a particular moonquake belt, or a region within a belt, tend to occur near the same tidal phase suggesting similar focal mechanisms. Deep moonquake magnitudes range from about 0.5 to 1.3 on the Richter scale with a total energy release estimated to be about 10^{11} ergs (10^4 J) annually. The largest shallow moonquakes have magnitudes of 4–5 and release about 10^{15}–10^{18} ergs (10^8–10^{11} J) each. Tidal deformation of a rigid lunar lithosphere overlying a reduced-rigidity asthenosphere leads to concentrations of strain energy near the base of the lithosphere. Although tidal strain energy can account for the deep moonquakes in this model, it cannot account for the shallow moonquakes. Tidal stresses within the lunar lithosphere range from about 0.1 to 1 bar (10^4–10^5 Pa). This low level of tidal stresses suggests that tides act as a triggering mechanism. The secular accumulation of strain implied by the uniform polarities of the deep moonquake signals probably results from weak convection. A convective mechanism could explain the distribution of moonquakes, the Earth-side topographic bulge, the distribution of filled mare basins, and the ancient lunar magnetic field.

Introduction

The Apollo seismic network includes stations installed at the landing sites of missions 12, 14, 15, and 16. It spans the near-face of the Moon in an approximate equilateral triangle with 1100 km spacing between stations (stations 12 and 14 are 181 km apart at one corner of the triangle (figure 1, plate 1). The oldest of these stations, Apollo 12, has now operated for six years, and the entire network has been in operation for 3.5 years as of November 1975.

Deep moonquakes have been detected by the long-period seismometers of each station at average rates of between 600 and 3000 per year, depending upon the station. An average of about five shallow moonquakes (high-frequency teleseismic events) have been detected annually. All of the deep moonquakes are quite small by terrestrial standards (Richter body-wave magnitude of 2 or less). The largest shallow moonquakes have Richter magnitudes of 4–5. The shallow and deep moonquakes are aligned in seismic belts of global extent suggesting the presence of a fundamental planetary tectonic mechanism.

Analysis of the siesmic signals from the man-made impacts and from moonquake and meteoroid impact sources has led to a model of lunar seismicity, structure, and tectonics that is quite different from that of the Earth (Latham *et al.* 1973; Lammlein 1973; Nakamura *et al.* 1973; Lammlein *et al.* 1974; Nakamura *et al.* 1974; Lammlein 1976). Refinements in the present model can be expected as data accumulate from natural events. In this brief review, the major findings to date regarding lunar seismicity, structure, and tecontonics from the Apollo passive seismic experiment are summarized.

Structure and state of the lunar interior

Zone I – the crust

The surface of the Moon is covered by a highly heterogeneous zone in which, probably owing to the nearly complete absence of volatiles, seismic waves propagate with very little attenuation. Scattering and low attenuation of seismic waves in this zone account for the prolongation of lunar seismic signals and the complexity of the recorded ground motion relative to typical terrestrial signals (Latham *et al.* 1973). Most of the scattering occurs in the outer several hundred metres, but significant scattering may occur to depths as great as 10–20 km. The 'granularity' within the scattering zone ranges from micrometre size fragments to heterogeneity on a scale of at least several kilometres. The roughness of the lunar surface primarily resulting from meteoroid impacts undoubtedly contributes to the scattering of seismic waves.

Analysis of the signals generated by the man-made impacts has revealed a major discontinuity at a depth of about 55 km in the eastern part of Oceanus Procellarum (Latham *et al.* 1973; Toksoz *et al.* 1972). By analogy with the Earth, we refer to the zone above the discontinuity as the crust, and to the zone below as the mantle. The seismic velocities of the lunar crust are appropriate for plagioclaise-rich minerals. Whether the crust is regional or global cannot be determined from the present seismic network. However, the early formation of a crust by igneous processes on a global scale would appear to explain such observations as the unexpectedly high heat flow (Langseth *et al.* 1972, 1973) and the presence of large scale petrological provinces inferred from orbital X-ray fluorescence data (Adler *et al.* 1972) and lunar sample analysis.

Zone II – the upper mantle

Analysis of travel-time data from the largest, distant meteoroid impacts (Nakamura *et al.* 1974), high-frequency teleseismic events (Nakamura *et al.* 1974), and deep moonquakes (Lammlein 1973, 1976; Lammlein *et al.* 1974) has revealed that the lunar interior below the crust is divided into four distinct zones, as shown in figure 2. The uppermost of these zones is the 250 km thick upper mantle. This zone extends from the base of the lunar crust to a depth of about 300 km and is characterized by a compressional wave velocity of about 8.1 km/s at the top, and possibly decreasing with depth. The Poisson's ratio is about 0.25. A mineral assemblage

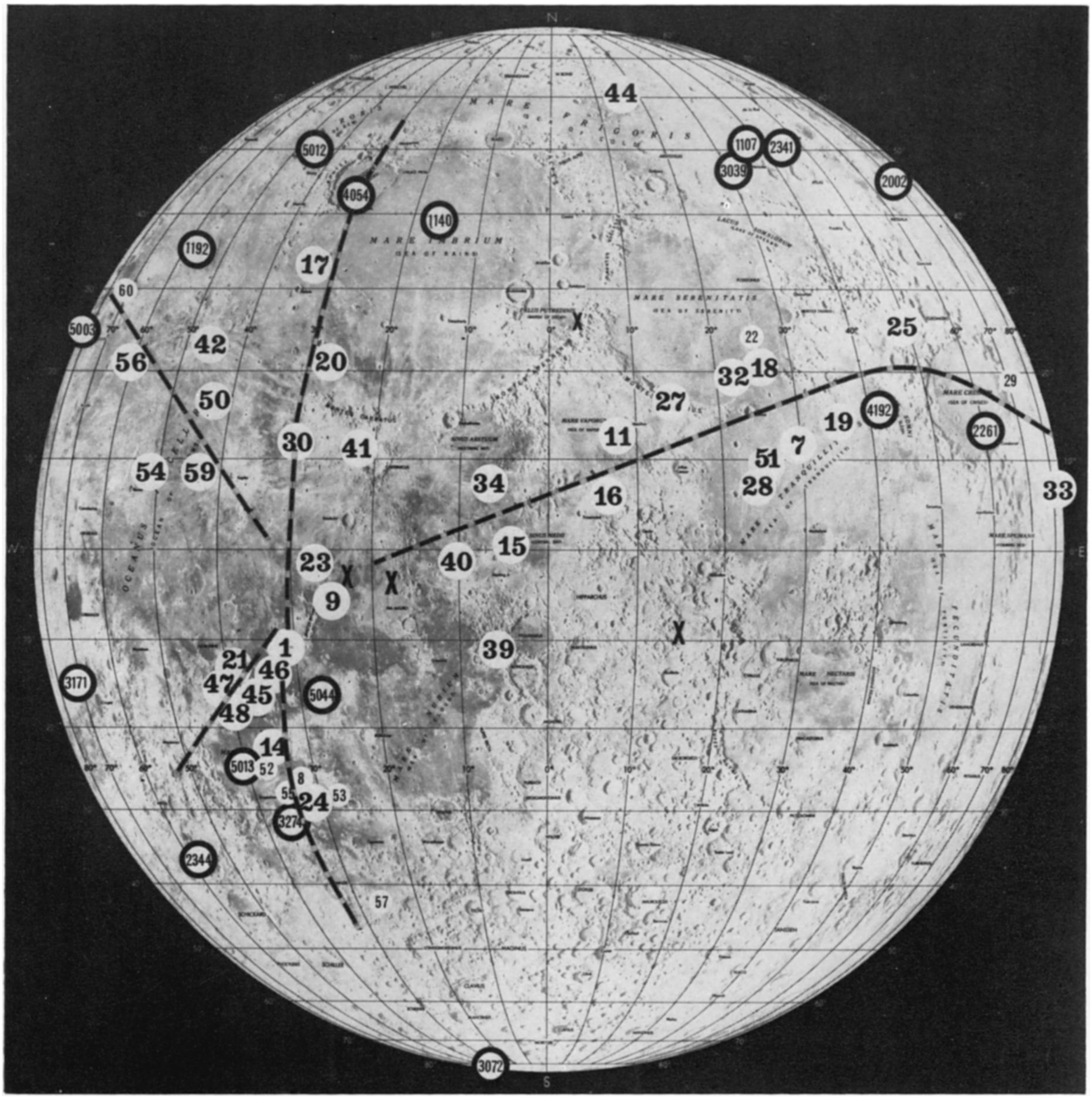

FIGURE 1. Map of the near-side of the Moon locating the Apollo 12, 14, 15 and 16 seismic stations and the deep and shallow moonquake epicentres. Large open circles indicate the foci for which depth can be determined. Small open circles correspond to cases in which data are insufficient for determination of depth. In these cases, depths of 900–1000 km were assumed to locate the epicentres. The numbers within the open circles identify the category A epicentres. Dark-ringed circles indicate the locations of the shallow moonquake (h.f.t.) epicentres. The first digit within a dark-ringed circle indicates the year in which the shallow moonquake occurred and the last three digits the day on which it occurred. Location circles on the edge of the lunar disk correspond to foci located on the far-side of the Moon.

(*Facing p.* 452)

consisting of olivine and pyroxene (Duba & Ringwood 1973) is consistent with the seismic data, although compositions richer in olivine than pyroxene are more probable, particularly near the top of this zone. An Mg/Mg-Fe ratio of 80 to 85 is inferred. The computed temperature gradients at the top of this zone are between 2 and 5 °C/km. Shallow moonquakes are concentrated in a 150 km thick zone at the base of the upper mantle (Lammlein 1976).

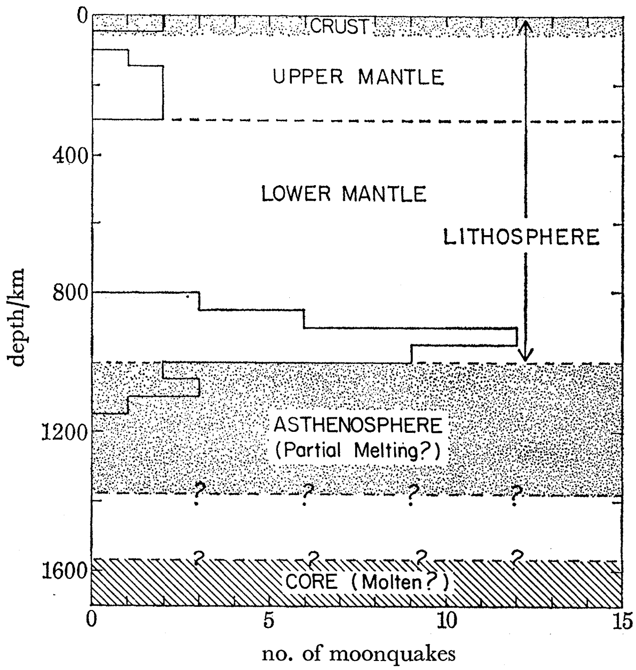

FIGURE 2. Radial section of the Moon showing the depth distribution of 9 shallow moonquake and 36 deep moonquake hypocentres and lunar structure. Deep moonquake activity is concentrated in a 200 km thick zone at the base of the lithosphere. Shallow moonquake activity is concentrated in a 150 km thick zone at the base of the upper mantle. No intermediate depth moonquakes have been identified.

Zone III – the middle mantle

This zone extends from about 300 km to about 1000 km depth and is characterized by reduced shear wave velocity. The Poisson's ratio increases with depth within this zone to an unusually high value of 0.33 to 0.36. This zone may represent primative lunar material below the zone of initial melting that produced Zones I and II (Duba & Ringwood 1973). Together the upper and middle mantle comprise the lithosphere. Deep moonquakes are concentrated in a 200 km thick zone at the base of the lithosphere (Lammlein 1976).

Zone IV – the lower mantle

The lower mantle begins at a depth of 1000 km and is characterized by high attenuation of shear waves. This zone is possibly partially molten, akin to the asthenosphere of the Earth.

Zone V – the core

This innermost zone has a radius of 170–360 km and is characterized by a greatly reduced compressional wave velocity. This zone may represent a completely molten core of iron sulphide (Brett 1972), although the present seismic data are too sparse to permit a strong case for this interpretation.

Lunar seismicity and tectonics

Moonquake occurrence characteristics

The Apollo seismic network detects several thousand deep moonquakes annually. Comparison has revealed that many of the long-period lunar seismic signals match each other in nearly every detail throughout the entire wavetrain. Sixty sets of matching events have been identified thus far by Lammlein (1976). Matching signals of each set are generated by repetitive moonquakes which occur at monthly intervals at one of sixty deep moonquake hypocentres. The repetition of seismic signals of identical waveforms indicates that each hypocentre remains fixed, to within about 10 km, and that the source mechanism does not change with time. The similarity between the signal character and occurrence characteristics of the more numerous weaker signals (category B) and the larger amplitude matching signals (category A) suggests that the smaller ones originate at or near the same hypocentres (Lammlein 1973, 1976; Lammlein *et al.* 1974). Together these deep moonquakes account for over 90% of the long-period seismic signals.

Moonquakes from individual hypocentres are detected for periods ranging from several months for the weakest sources to several years or more for the strongest sources, such as the A_1 moonquake hypocentre. During an active period one moonquake from an individual hypocentre is detected each month near a characteristic phase of the lunar tidal cycle. In several cases two to four moonquakes are detected each month within a 1–4 day interval. Slight differences among the signals from each of these hypocentral regions allow us to identify two to about twelve (A_1) closely spaced hypocentres that form an active zone. The linearity of the moonquake belts and the similarity of signals from these adjacent hypocentres suggests that the moonquake hypocentres define active fault segments parallel to the trend of the moonquake belts (Lammlein 1976).

The largest moonquakes from a given hypocentre occur when the lunar tides best match the characteristic phase of that hypocentre. The signal amplitudes generally decrease with time before and after the characteristic phase. In all cases the characteristic tidal phase is determined by the relative phases of the anomalistic and nodical months. Because a given phase relation between the anomalistic and nodical months occurs at intervals of six years, the largest moonquakes from a given hypocentre should occur every six years. Lammlein *et al.* (1974) and Lammlein (1973) predicted a six-year cycle in A_1 moonquake activity based upon the secular decline in A_1 activity and its exact correlation with the anomalistic-nodical month cycle. They predicted that large A_1 moonquakes would again be observed in 1975–6. Lammlein (1976) reports that large amplitude A_1 moonquake signals were detected in 1975 indicating the initiation of a new cycle of activity. The largest A_1 moonquakes should occur in early 1976 when the characteristic phase of the A_1 moonquake hypocentre occurs again. Because all of the deep moonquakes are tidally controlled we may now predict this same type of resurgence for all of the deep moonquakes.

The monthly repetition of moonquake signals is easily understood because the lunar tides differ only slightly from month-to-month. However, this difference increases with time providing an explanation of the observed buildup and decline of moonquake signal amplitudes about the characteristic phase. The $7\frac{1}{2}$ anomalistic month variation in moonquake signal amplitudes results from the fact that the phase relations between the anomalistic and nodical months are very similar at $7\frac{1}{2}$ month intervals.

The fact that deep moonquakes occur with periodicities of one anomalistic month, one nodical month, $7\frac{1}{2}$ anomalistic months, and six years, and that their occurrence times and energy release characteristics are well correlated with specific phases of the lunar tidal cycle implies that lunar tides are the dominant controlling mechanism of deep moonquake activity.

Hypocentral locations of deep and shallow moonquakes

Signals from 36 deep moonquake foci provide the body wave data necessary to compute hypocentral locations. Epicentral locations can be determined in 7 additional cases if focal depths are assumed. These arrival time data are derived from the detailed analysis of a data set of nearly 1000 individual moonquakes detected by the seismometers at three or four stations, a total of several thousand moonquake signals. Because each moonquake source repeatedly produces nearly identical signals, we have stacked the signals of nearly all events recorded more than 10 times at any of the seismic stations. This results in a signal-to-noise enhancement of 3 or more and enables us to confidently identify the P and S phase arrivals in nearly every case. Hence, the present data set is more extensive and reliable than those used previously, and is the best possible at this time.

Lammlein *et al.* (1974) and Lammlein (1973) discovered a western belt of moonquake activity trending nearly north–south and an eastern belt trending east–northeast to west–southwest, both about 2000 km in length and lying along arcs of great circles. The present distribution of moonquake epicentres also defines distinct belts although greater detail is now evident in the old belts and a new belt can now be identified as shown in figure 1.

The moonquake epicentres of figure 1 define three major moonquake belts: a western belt trending nearly north–south from the A_{17} epicentre to the A_{57} epicentre, an eastern belt trending east–northeast to west–southwest and extending from the A_{33} epicentre to the A_{40} epicentre and possibly intersecting the western belt at a point on the lunar equator at 25° west longitude, and finally a newly discovered northwestern belt trending northwest to southeast and extending from the A_{60} epicentre to the A_{59} epicentre. The northwestern belt may intersect the eastern and western moonquake belts in central Oceanus Procellarum. The A_{44} epicentre in Mare Frigorus is an isolated, but well located, zone of moonquake activity that suggests a fourth moonquake belt.

The distribution of moonquake epicentres within the major belts suggests that each is composed of several minor belts that connect to form seismic zones of global extent. The similarity of occurrence characteristics of the moonquake sources within each minor belt supports this hypothesis (Lammlein 1976).

Nakamura *et al.* (1974) have described the small number of h.f.t. (high-frequency teleseismic events) seismic signals that are much richer in high frequencies than other events observed at comparable distances, and display relatively impulsive P- and S-wave beginnings indicating negligible scattering near the source. Because the h.f.t. waveform characteristics resemble those of the deep moonquakes and their source depths could range from 0 to 300 km, Nakamura *et al.* (1974) favoured the hypothesis that the h.f.t. events are shallow moonquakes. The strong similarities between the deep category A moonquake and h.f.t. epicentral locations and occurrence time chacteristics now available require that the h.f.t. events are shallow moonquakes (Lammlein 1976). The epicentral locations of 17 of the 20 shallow moonquakes identified to date are mapped in figure 1. The arrival time data used in calculating the shallow moonquake source locations shown in figure 1 are from Lammlein (1976) and are very similar to that obtained by Nakamura *et al.* (1974).

In general, the shallow moonquake source locations are not as accurate as those of the deep moonquakes. Many of the shallow moonquakes are small or are well-recorded at only two or three stations and 9 of the 17 events are located with data from only one or two stations. Consequently, the locations of the most distant or smallest events could be in error by as much as 5–10°.

It is noteworthy that the shallow moonquakes show a spatial distribution that is very similar to that of the deep moonquakes, as shown in figure 1. Five of the shallow moonquake epicentres lie along the deep moonquake belts and an additional 10 occur within 10–30° of deep moonquake belts. Shallow moonquakes are associated with each of the three major moonquake belts and also the A_{44} seismic zone.

The depth distributions of the deep and shallow moonquakes are shown in figure 2 superimposed upon the lunar structural model discussed earlier. The 36 deep moonquake focal depths range between 800 and 1150 km with two-thirds of the hypocentres falling in the narrow range of 850–1000 km depth. The average depth for all of the 36 deep moonquakes is 943 km. This range and distribution of focal depths is nearly identical to that of Lammlein (1973) and Lammlein *et al.* (1974). As shown in figure 2, the hypocentral depths of 9 shallow moonquakes range from 0 to 300 km with two-thirds of the hypocentres falling in the range of 150–300 km depth. Thus, we find deep moonquakes concentrated within a narrow 200 km depth range at the base of the lunar lithosphere, no intermediate depth moonquakes in the range of 300–800 km depth, and shallow moonquakes concentrated in a 150 km depth range at the base of the lunar upper mantle.

Lunar tectonics

Reliable earthquake focal mechanisms require observations of the polarities of body waves at numerous seismic stations covering a large range of azimuths and distances with respect to the epicentre. However, lunar results are severely limited by the small number of seismic stations, the intense scattering of lunar seismic signals, and the low energy of the moonquakes recorded to date. Thus, data are insufficient to calculate fault plane solutions, but the following observations bear on the nature of the focal mechanism.

(i) *Polarities of seismic signals.* With very few exceptions, the polarities in a set of matching events are identical. This implies that the dislocation is progressive. Progressive dislocations suggest secular accumulations of strain periodically released by the deep moonquakes. The fact that each shallow moonquake is a unique, non-repeating event suggests that the shallow moonquakes also release secular accumulations of strain energy.

An unusual feature of the A_1 moonquake history is that signals closely resembling inverted A_1 moonquake signals, hence called $A_{1(I)}$ for A_1 inverted, were observed in 1972–3. This $A_{1(I)}$ family is thus 3 years, or $\frac{1}{2}$ of the six-year tidal cycle, out-of-phase with the main family of A_1 moonquakes. These $A_{1(I)}$ signals can be interpreted as representing motion along the A_1 fault segment in the opposite sense of the usual displacement or motion along a fault perpendicular to the A_1 fault segment. The possibility of reverse motions would not significantly affect the net cumulative displacement because the main family of A_1 moonquakes is much more numerous and energetic.

(ii) *Matching waveforms.* The persistence of matching waveforms implies that the locations of each focal zone must remain fixed to within about 10–20 km or less for periods as long as several years. The dozen subgroups of A_1 signals suggests that the A_1 source region may extend over a distance of some 30 km and connect with its adjacent hypocentres in the western moonquake belt (Lammlein 1976).

(iii) *Shear wave*. The prominence of shear waves in the shallow and deep moonquake signals suggests that, like earthquakes, moonquakes are shear dislocations.

(iv) *Signal spectra*. The flatness of deep moonquake spectra (Lammlein *et al.* 1974) and shallow moonquake spectra (Nakamura *et al.* 1974) suggests fault dislocations by comparison with Brune's (1970) analysis of earthquake spectra.

(v) *Cumulative amplitudes*. Cumulative amplitude distributions of deep moonquakes yield slopes of 1.5–4.0 (Lammlein 1976) and those of shallow moonquakes slopes of about $\frac{1}{2}$ (Nakamura *et al.* 1974). The slope values for the deep moonquakes are then significantly higher than the value of about 1.0 normally observed for tectonic earthquakes, while the shallow moonquakes values are slightly lower. As shown by Lammlein *et al.* (1974), this high slope value for the deep moonquakes results from the tidal controlling mechanism. Similarly, the less exact correlation between the shallow moonquake occurrence characteristics and lunar tides could also explain why the shallow moonquake distributions have normal slope values.

(vi) *Moonquake energy release and magnitudes*. Lammlein *et al.* (1974) and Lammlein (1973) report that the largest deep moonquakes have Richter magnitudes of about 1.3 and the smallest about 0.5. They conclude that the annual lunar seismic energy release from deep moonquakes is of the order of 10^{11} erg (10^4 J). The largest shallow moonquakes have Richter magnitudes of about 4–5 corresponding to a seismic energy release of about 10^{15}–10^{18} erg (10^8–10^{11} J). Because the cumulative distribution slope of the shallow moonquakes is 0.5, the single largest shallow moonquake each year will account for most of the seismic energy released by these events.

(vii) *Available tidal energy*. Lammlein (1976) has shown that if a weak, low-rigidity core or shell exists below the lithosphere in a moon subjected to tidal deformation, tidal strain energy density reaches a local maximum in the 200 km thick zone at the base of the lithosphere (figure 3). A minimum strain energy density of 0.1 erg/cm^3 or 10^{14} erg/km^3 would occur in this region. The largest deep moonquake releases about 10^9 erg of seismic energy. If we assume a focal region of 1 km^3 and that 1 % of the available tidal strain energy is converted to seismic wave energy, the total amount of strain energy released by a moonquake would be 10^{11} erg, far below the available tidal strain energy of 10^{14} erg. This suggests that the dissipation of tidal energy by deep moonquakes is a reasonable hypothesis, especially since the deep moonquakes are concentrated in this zone.

A difficulty arises when considering the shallow moonquakes. The largest shallow moonquake has a seismic energy release of about 10^{15}–10^{18} erg. Even allowing for a relatively large focal region of 1000 km^3 and a 100 % conversion of tidal strain energy to seismic waves (i.e. no energy available for fracturing rock, heat, etc.) the tidal strain energy would barely be sufficient to account for the shallow moonquakes. This is because strain energy density approaches zero near the lunar surface. By using a typical strain energy density of 0.05 erg/cm^3, the available deformational energy would be 5×10^{16} erg per shallow moonquake. This would require an exact conversion of all of the available tidal energy to seismic energy. A more realistic 1 % conversion of tidal to seismic energy would leave 5×10^{14} erg per moonquake. Hence we must conclude that the shallow moonquakes release a significant amount of strain energy resulting from tectonic activity. Becuase of their tidal correlations with the deep moonquakes it appears that the shallow moonquakes are triggered by lunar tides.

(viii) *Moonquake occurrence characteristics.* As discussed earlier, the identification of the many tidal periodicities in the occurrence and energy release characteristics of the deep moonquakes implies that lunar tides control deep seismic activity. In addition, the moonquakes from a given hypocentre tend to occur near a characteristic phase of the tidal cycle. As suggested by the limited earlier data (Lammlein *et al.* 1974; Lammlein 1973), many of the deep moonquake hypocentres posses similar and often nearly identical occurrence characteristics. A most significant feature of these groupings is that the epicentres of these moonquakes group together in a very similar manner (Lammlein 1976). Thus, we find that deep moonquakes of a particular moonquake belt, or a region within a belt, all occur near the same characteristic tidal phase.

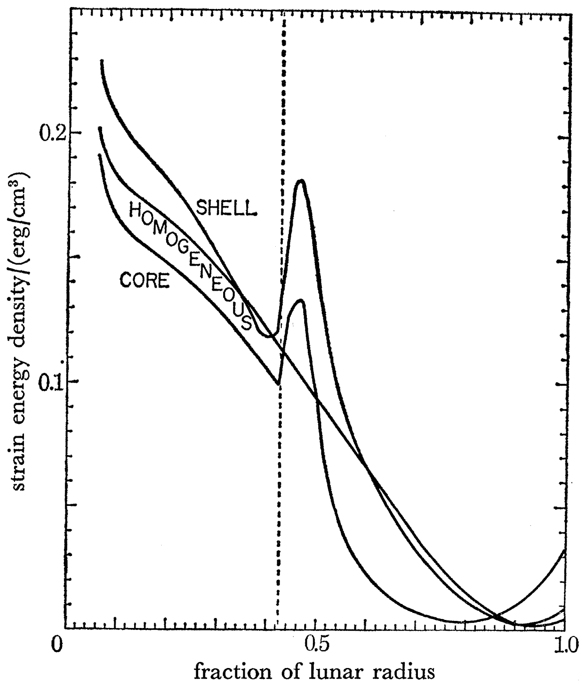

FIGURE 3. Radial section of the Moon showing strain energy density profiles for three lunar models. In each case, strain energy decreases from a maximum at the centre of the Moon to a minimum at depths of 100–400 km below the lunar surface. A local maximum in tidal strain energy density occurs within the reduced-rigidity zone of the shell model and in the reduced-rigidity core-mantle transition zone of the core model. The dotted line marks the radius of the low-rigidity core and the axis of the low-rigidity shell.

In addition, the shallow moonquakes of a given region also tend to occur near the same tidal phase as the deep moonquakes in that region. The fact that all of the moonquakes of a given seismic belt tend to occur at the same tidal phase suggests that nearly identical fault motion occurs at each hypocentre.

(ix) *Tidal stresses.* One of the most important clues bearing on the nature of moonquake focal mechanisms is the orientation of the tidal stresses at individual moonquake hypocentres when moonquakes occur. With very few exceptions, deep moonquakes of the eastern, western, and northwestern belts occur at characteristic tidal phases that correspond to an alignment of two of the principal tidal stresses in a vertical plane that is in or at a 45° angle with the vertical plane containing their respective moonquake belt (Lammlein 1976). The third principal stress is horizontal and in or at 45° with the vertical plane containing the moonquake belt. The fact that such a stress alignment relative to the seismic belts is critical to the occurrence of the deep moonquakes supports our hypothesis that moonquakes are shear dislocations along fault planes approximately parallel to the trends of the moonquake belts.

Typical tidal stresses at the depth of the deep moonquakes are within the range of 0.1–1 bar (10^4–10^5 Pa), as shown in figure 4. Stresses of this magnitude are insufficient to generate moonquakes in unfractured rock, implying that the tidal stresses cause dislocations along pre-existing fracture planes or act as a triggering mechanism.

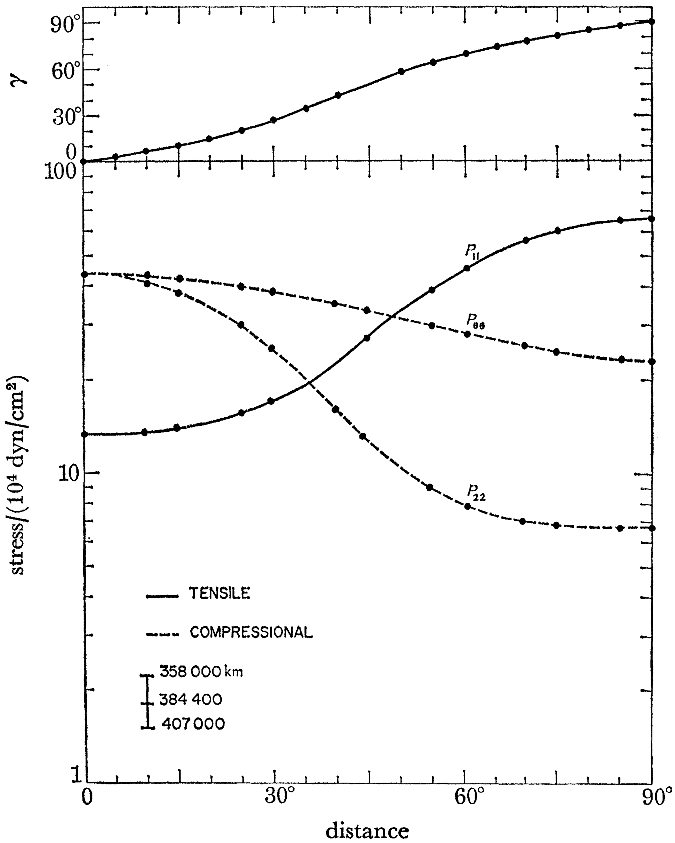

FIGURE 4. Principal tidal stresses at a depth of 938 km in the Moon plotted as functions of angular distance from the subearth point. The tidal stresses shown occur near the base of a lunar lithosphere overlying a reduced-rigidity core. $P_{\theta\theta}$, P_{11}, P_{22} form an orthogonal system with $P_{\theta\theta}$ always horizontal and oriented perpendicular to any great circle containing the subearth point. P_{11} and P_{22} are contained within the great-circle plane. The angle γ is measured from the vertical to P_{11} in the direction towards the subearth point. Maximum shear stresses occur along planes oriented at 45° angles to the pairs of principal stresses and have amplitudes of one-half the difference between the pairs of principal stresses.

As shown in figure 4, the greatest compressive stress, $P_{\theta\theta}$, is always horizontal. The intermediate stress, P_{22}, is always compressive and the least compressive stress, P_{11}, is always tensile. Most of the deep moonquake hypocentres occur within 45° of the centre of the lunar disk. At these locations the least compressive stress is within 45° of the vertical and the intermediate within 45° of the horizontal.

Preliminary analysis of tidal stresses at the times and locations of moonquake occurrence reveals that moonquakes are most probably thrust or reverse faulting events (Lammlein

1976). These types of faulting are favoured because predominately horizontal, compressive stresses appear to control the occurrences of deep moonquakes. In addition, the importance of compressive stresses for the occurrence of moonquakes may explain two basic features of lunar seismicity – the absence of intermediate depth moonquakes and the lack of any shallow moonquakes within 30° of the centre of the lunar disk. Compressive stresses within the lunar lithosphere decrease from a maximum at the depths of the deep moonquakes to a minimum near the lunar surface. At the depths of the shallow moonquakes there are no compressive tidal stresses within about 35° of the centre of the lunar disk. Thus, shallow moonquakes only occur in regions characterized by compressive tidal stresses. If sufficient strain energy for moonquake occurrence is stored at intermediate depths, then the tidal compressive stresses are too small to trigger moonquakes in that region.

Discussion and conclusions

According to our present model, the Moon is characterized by a thick, rigid outer shell, the lithosphere, surrounding a weaker zone, the asthenosphere, in which partial melting is probable. If so, temperatures near 1500 °C are probable. The lithosphere is divided into three layers – the crust, the upper mantle, and the middle mantle. A small core may be present below the asthenosphere. Like earthquakes, moonquakes are distributed in two major belts of global extent that coincide with the regions of youngest and most active volcanic and tectonic activity. Deep moonquakes are small, closely correlated with tides, and could represent the dissipation of tidal energy. Shallow moonquakes, although also correlated with tides, are much more energetic than the deep moonquakes and require a source of tectonic strain energy. The similarities in the distribution and occurrence characteristics of both deep and shallow moonquakes suggests that this tectonic mechanism accounts for all of the lunar seismic activity. Lunar tidal stresses act as an effective triggering mechanism for moonquakes because of the low level of lunar tectonic activity and the great thickness of the lunar lithosphere. The uniform polarity of matching signals from individual hypocentres indicates that cumulative tectonic strain energy is being released by the moonquakes.

Possibly the moonquakes define the trends of major fracture systems created by the mare forming impacts. These fracture systems would still be present at the depths of the deep moonquakes if that zone is composed of primative lunar material below the zone of initial melting. Such a fracture system may also be partially preserved near the lunar surface in regions devoid of mare material because the large impacts post-date the formation of the lunar crust. In this model, deep and shallow moonquakes might occur along these pre-existing fractures, or lines of structural weakness in response to present day tectonic stresses. Intermediate depth moonquakes would be absent, as observed, because fractures in that depth range have probably been destroyed by the melting process that produced the mare basalts. A fundamental difficulty with this hypothesis is that moonquake activity would be concentrated near the largest impact basins. This is not the case, although the eastern moonquake belt is subparallel to the trend of the near-side, ringed basins and its location may be influenced by these features.

Runcorn (1974) demonstrated that groups of elevation points on the highlands, circular maria, and irregular maria all fit ellipsoids of similar ellipticity with their long axes pointing to the earth at nodal passage. He found that the height of the earth-side 'bulge' is over 3 km, more than twice as great as that inferred by the differences in moments of inertia. These data then suggest that there is a variation of density over level surfaces in the lunar interior which would be entirely consistent with the convection pattern postulated by Runcorn (1967). An internal convection mechanism would maintain a bulge that otherwise would have been dissipated by solid state creep during the last 3 Ga. The fact that the moonquake focal mechanisms favour thrust faulting suggests that the amplitude of convection is decreasing, perhaps due to cooling. This decrease presumably would be associated with a decreasing amplitude lunar magnetic field.

In addition to maintaining the earth-facing topographic bulge, an asymmetric convective system that is upwelling on the near-side and downwelling on the far-side could explain why only the near-side mare basins have been filled. This convective system could also account for the pattern of lunar seismic activity. An upwelling convective cell in central Oceanus Procellarum could generate tectonic stresses of sufficient magnitude to account for the moonquake belts that radiate from that region of the Moon. The low-level of energy release by the moonquakes suggests a weak convective mechanism for the Moon in comparison to that of the Earth.

Comparison of the moonquake epicentre map of figure 1 and the lunar transient event map of Middlehurst (1967) reveals that the surface distributions of both groups are very similar. The shallow and deep moonquake epicentres and the lunar transient event sites are concentrated in three near-side lunar quadrants with few transients and no moonquakes occurring in the southeast highlands quadrant. Although we have found no correlation between the locations or occurrence times of individual moonquake and transient events, both moonquakes and transients are tidally controlled and reflect present-day lunar tectonic activity.

This work was supported by the National Aeronautics and Space Administration under contract NAS 9-13143 at the Marine Science Institute, University of Texas, Galveston, Texas.

References (Lammlein)

Adler, I., Trombka, J., Gerard, J., Lowman, P., Schamdebeck, R., Blodget, H., Elller, E., Yin, L., Lamothe, G., Osswald, G., Gorenstein, P., Bjorkholm, P., Gursky, H., Harris, B., Galub, L. & Harnden, F. R. 1972 *NASA Spec. Publ. SP-315*, sect. 19, **1**.

Brette R. 1972 *Trans. Am. Geophys. Un.* **53**, 723.

Brun,, J. 1970 *J. geophys. Res.* **75**, 4997–5009.

Duba A. & Ringwood, A. E. 1973 *The Moon* **7**, 356–376.

Lammlein, D. R. 1973 Doctoral Dissertation, Columbia University, 1–99.

Lammlein, D. R. 1976 *Lunar seismicity and tectonics* (in preparation).

Lammlein, D. R., Latham, G. V., Dorman, J., Nakamura, Y. & Ewing, M. 1974 *Rev. Geophys. Space Phys.* **12**, 1–21.

Langseth, M., Clark, S., Chute, J. & Keihm, S. 1972 *NASA Spec. Publ. SP-289, sect.* **11**.

Langseth, M., Chute J. & Keihm, S. 1973 (abstract), in *Abstracts of the Fourth Lunar Science Conference*, edited by J. W. Chamberlain & C. Watkins, pp. 455–456, Lunar Science Institute, Houston, Texas.

Latham, G. V., Ewing, M., Dorman, J., Nakamura, Y., Press, F., Toksoz, N., Sutton, G., Duennebier, F. & Lammlein, D. 1973 *Moon* **1**, 272–296.

Middlehurst, B. M. 1967 *Rev. Geophys.* **5**, 173–190.

Nakamura, Y., Dorman, J., Duennebier, F., Ewing, M., Lammlein, D. & Latham, G. 1974 *Proc. 5th Lunar Sci. Conf., Geochim. cosmochim. Acta, Suppl.* 5, **3**.

Nakamura, Y. N., Lammlein, D., Latham, G., Ewing, M., Dorman, J., Press, F. & Toksoz, N. 1973 *Science, N.Y.*, **181**, 49–51.

Nakamura, Y. N., Latham, G., Lammlein, D., Ewing, M., Duennebeir, F. & Dorman, J. 1974 *Geophys Res. Lett.* **1**, 137–140.

Runcorn, S. K. 1967 *Proc. R. Soc. Lond.* A **296**, 270–284.

Runcorn, S. K. 1974 *Proc. R. Soc. Lond.* A **336**, 11–33.

Toksoz, M. N., Press, F., Anderson, K., Dainty, A., Latham, G. Ewing, M., Dorman, J., Lammlein, D., Sutton, G., Duennebier, F. & Nakamura, Y. 1972 *Science, N.Y.* **176**, 1012–1016.